Analysis of the Spatiotemporal Dynamics and Drivers of Ecosystem Health in Xinjiang

Xiaming Yang, Renping Zhang , Jing Guo, Liangliang Zhang, Xueping Gou, Zhengjie Gao, and Xuewei Liu

Abstract—**Ecosystem health is a key indicator of regional sustainable development and is important for guiding regional ecological improvement. However, long-term time-series analyses of ecosystem health, its drivers, and changes related to future trends have not yet been adequately carried out. Xinjiang, a typical Central Asian arid region, is taken as a case study, and an indicator system based on the driver–pressure–state–impact–response model is established. Then, an ecosystem health assessment method using the TOPSIS model with the combined weighting method is proposed, and the determinants influencing the health of ecosystems are scrutinized utilizing the geographical detector approach and the geographically weighted regression model. Finally, the future trend of ecosystem health change was predicted by applying the Hurst exponent combined with slope trend analysis. The findings reveal the following observations: First, between 2000 and 2020, the zones in Xinjiang demonstrating robust ecosystem health predominantly encompassed the Altai Mountains and areas proximal to the Tian Shan Mountains; the low-value regions were concentrated in the Junggar Basin and around the Tarim Basin; and the areas with an improved ecosystem health index accounted for 92.1% of the research zone. Second, natural driving factors dominate the research zone. Dominant drivers vary among regions and are affected by interactions between multiple factors, with positive and negative effects. Third, in the designated study area, regions exhibiting an increase and persistent trend in ecosystem health are projected to constitute 85.05% of the total area. This research is promising for providing decision support and a case for sustainable development in Xinjiang.**

Index Terms—**Driving factor, ecosystem health, TOPSIS model, Xinjiang.**

I. INTRODUCTION

ECOSYSTEM health refers to the ability of an ecosystem to sustain structural integrity and functional equilibrium, concurrently providing ecological services advantageous to human society [1]. Healthy ecosystems are not only beneficial for human existence; they also foster a harmonious balance between ecological safety and socioeconomic well-being [2]. However, increasing human activities and drastic changes in the global climate have caused ecosystems to deteriorate [3]; forest reduction, desert expansion, grassland degradation, soil erosion, and species extinction are occurring increasingly frequently [4], [5], [6], with serious impacts on ecosystem health. Remote sensing technology is essential for effectively monitoring ecosystem changes and assessing their health status. It enables effective monitoring of ecosystem changes, including indicators, such as vegetation cover and biomass, providing data support for assessing ecosystem health. Combined with technologies, such as geographic information system (GIS), remote sensing also enables comprehensive research on the spatial distribution and dynamic changes in ecosystems, providing more thorough and precise data support for ecosystem health evaluations.

In recent years, studies on ecosystem health have primarily focused on three areas, starting with ecosystem health assessment methods. The choice of assessment methods is crucial in ecosystem health evaluations due to the complexity of ecosystems. Many researchers have adopted different assessment methods from various perspectives, including widely used methods, such as the pressure–state–response model [7], vitality–organization–resilience model [8], Vigor–organization–resilience–services [9], and landscape ecological models [10]. Many of the aforementioned models emphasize simplifying internal system relationships, while the driving forces–pressures–state–impacts–responses (DPSIR) framework is acknowledged as the primary approach for establishing indicators of ecosystem health [11]. The DPSIR model substantially improves upon traditional qualitative approaches, providing a more accurate depiction of the dynamics and interactions among elements in complex ecosystems [12], [13]. The second area of focus is the driving forces behind ecosystem health. Identifying how various factors influence ecosystem health and exploring the spatial diversity of these drivers are crucial for policymakers to formulate risk-reduction strategies and effectively allocate resources. Currently, researchers are choosing different typical areas to study how natural environmental factors (such as topography, climate, and hydrology) and human socioeconomic factors (including population, urbanization, environmental pollution, land use, and regional policies) linearly and spatially heterogeneously impact ecosystem health [14], [15], [16], [17], using methods, including principal component analysis (PCA) [18], regression analysis [19], geodetector models [9], and geographically weighted regression (GWR) models [20]. The

Xiaming Yang, Renping Zhang, Liangliang Zhang, Xueping Gou, Zhengjie Gao, and Xuewei Liu are with the Key Laboratory of Oasis Ecology, College of Ecology and Environment, Xinjiang University, Urumqi 830046, China (e-mail: 107552201191@stu.xju.edu.cn; zhrp@xju.edu.cn; 107552203756@stu.xju.edu.cn; 2503557943@qq.com; 1055359788@qq.com; 107552201196@stu.xju.edu.cn).

Jing Guo is with the Xinjiang Academy Forestry, Urumqi 830000, China (e-mail: lkyguojing@gmail.com).

third focus is on predicting future changes in ecosystem health. Forecasting future ecosystem health lays a solid foundation for the formulation of environmental policies. However, most existing studies tend to concentrate on assessing the health of regional ecosystems from historical and present perspectives, frequently overlooking future predictions and analyses. The uncertainty of human activities and the complexity of ecosystems make it difficult to predict future ecosystem health condition. Facing such challenge, some researchers still make forecasts about future trends, such as the authors in [20] and [21], who, based on future development scenarios, found that ecological transformation is key to improving resource-depleted cities; Xiao et al. [22] used the hidden Markov model to monitor and predict the health of urban agglomerations' ecosystems.

To date, numerous studies on ecosystem health assessment have been conducted at various scales, including provinces [23], major cities [24], urban agglomerations [25], [26], rivers [27], [28], wetlands [29], and forests [30]. Situated at the core of the Eurasian continent, Xinjiang exemplifies the arid and semiarid terrains characteristic of the Central Asia region [31]. In recent years, while Xinjiang has experienced rapid socioeconomic growth and a sharp population rise, its ecosystem remains relatively fragile and faces serious threats under harsh natural conditions and various pressures from human activities [32]. In this context, numerous studies have targeted Xinjiang or specific regions within this region. Evaluations of the entire region have primarily focused on aspects, such as habitat quality [33], resource and environmental carrying capacity [34], ecological risk assessment and forecasting [35], ecosystem service values (ESVs) [36], ecological security patterns [37], and ecosystem resilience [38]. Meanwhile, studies focusing on specific parts of Xinjiang have covered topics, such as the ESVs of the Tarim River basin [39], the ecosystem service assessment of the Manas River [40], the ecosystem health of southern Xinjiang [41], and ecosystem services in northern Xinjiang [42].

However, upon reviewing the existing research, several deficiencies in studies conducted in Xinjiang are highlighted.

1) Comprehensive assessments of the region's ecosystem health are rare, and previous studies usually determine indicator weights based solely on subjective or objective methods.
2) In terms of the drivers of ecosystem health, currently, most studies explore the impact of individual factors on the entire study area, with little focus on the spatial variability of these drivers.
3) Studies predicting future ecosystem health are still rare.

In summary, to make up for the lack of research on ecosystem health in Xinjiang, this study is based on widely collected remote sensing data and statistical data. The main research objectives are as follows:

1) proposing an ecosystem health assessment framework based on the DPSIR-TOPSIS model and a comprehensive weighting approach;
2) exploring the drivers affecting ecosystem health in Xinjiang and the spatial variability of dominant drivers;
3) predicting the future trend of ecosystem health in Xinjiang based on the Hurst exponent and slope trend analysis methods.
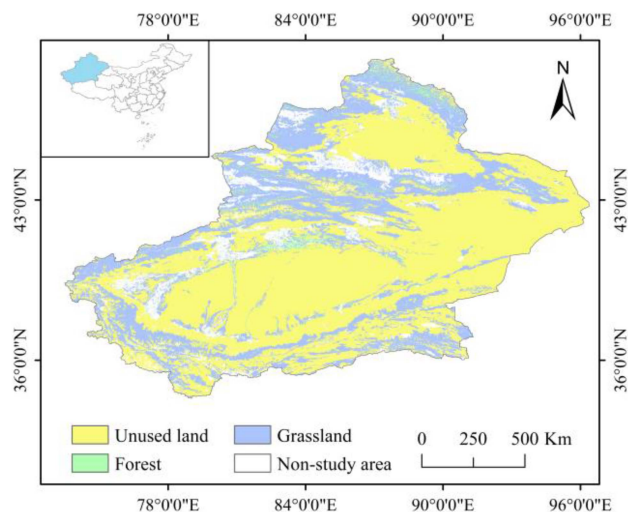

Fig. 1.   Geographic location of Xinjiang.

II. MATERIALS AND METHODS

A. Study Area

Situated in the northwestern part of China, Xinjiang spans longitudes from 73°40′E to 96°18′E and latitudes from 34°25′N to 48°10′N (see Fig. 1). Xinjiang's topography is characterized by a distinctive pattern known as "three mountains and two basins." The region's average elevation is approximately 1000 m. This special geographic location has given the region unique climatic characteristics; it has the largest mobile desert and semifixed deserts in China [43], with an average yearly rainfall of approximately 130 mm, contrasted with an annual evaporation rate exceeding 1000 mm. Given that Xinjiang is distant from any oceanic coastline and encircled by mountain ranges, it is difficult for oceanic air currents to reach the region; additionally, the natural conditions of low precipitation and high evaporation, as well as human activities, seriously threaten the ecosystem health of the region.

B. Data Sources and Description

There are two types of data (spatial and statistical data, Table I) involved in this article. Data preprocessing and calculations were primarily conducted using ArcGIS 10.8 and Microsoft Excel. Vegetation cover and biomass were calculated with reference to [44] and [45], respectively.

C. Research Methods

The study included the following steps.

1) Utilizing the DPSIR framework, this study comprehensively evaluated both natural environmental factors and human activities. An ecosystem health assessment index system was established employing a combined weighting approach. Furthermore, the TOPSIS model was implemented to quantitatively evaluate the ecosystem's health status.

TABLE I
DATA SOURCES AND DESCRIPTION

Data type	Name of data	Data sources	Scale
Spatial data	population density	WoldPop(https://www.worldpop.org)	1000 m
	average annual temperature	The Resource and Data Sharing Center of the Chinese Academy of Sciences (http://www.resdc.cn/DataList.aspx)	1000 m
	average annual rainfall	The Resource and Data Sharing Center of the Chinese Academy of Sciences (http://www.resdc.cn/DataList.aspx)	1000 m
	nighttime light	The Resource and Data Sharing Center of the Chinese Academy of Sciences (http://www.resdc.cn/DataList.aspx)	1000 m
	total evapotranspiration	National Earth System Science Data Center(http://www.geodata.cn)	1000 m
	slope	Geospatial data cloud(https://www.gscloud.cn/)	90 m
	slope direction	Geospatial data cloud(https://www.gscloud.cn/)	90 m
	altitude	Geospatial data cloud(https://www.gscloud.cn/)	90 m
	vegetation cover	[44]	1000 m
	soil carbon content	Food and Agriculture Organization of the United Nations (https://www.fao.org/home/en)	3000 m
	soil pH	Food and Agriculture Organization of the United Nations (https://www.fao.org/home/en)	3000 m
	soil nutrient availability	Food and Agriculture Organization of the United Nations (https://www.fao.org/home/en)	3000 m
	biomass	[45]	1000 m
Statistical data	amount of tourism revenue	Xinjiang Statistical Yearbook	/
	livestock number	Xinjiang Statistical Yearbook	/
	electricity consumed by residents	Xinjiang Statistical Yearbook	/
	primary industry	Xinjiang Statistical Yearbook	/
	per capita disposable income	Xinjiang Statistical Yearbook	/
	level of grain production	Xinjiang Statistical Yearbook	/
	area of soil and water erosion control	Xinjiang Statistical Yearbook	/
	number of schoolchildren	Xinjiang Statistical Yearbook	/
	total value of the tertiary industry	Xinjiang Statistical Yearbook	/

2) This study examined the spatial and temporal distribution patterns of ecosystem health and delineated the trajectory of its center of gravity across various health levels.

3) This research investigated the determinants of ecosystem health by employing both the geodetector model and the GWR model.

4) The projection of future trends in ecosystem health was conducted by integrating the Hurst exponent with slope trend analysis.

1) Construction of the Indicator System: As a major pastoral area, grazing activities have had a considerable impact on the ecosystem health in Xinjiang [46]; in recent years, the tourism industry in Xinjiang has developed rapidly [47]; additionally, this region is characterized by significant evapotranspiration [48] and poor soil conditions. However, such factors have rarely been considered in previous studies. Thus, this research adopts indicators, including the number of livestock, tourism income, total evapotranspiration, and soil physicochemical properties, to comprehensively evaluate the ecosystem's health status.

In this article, the DPSIR model was chosen to divide all the indicators into five main categories, namely, drivers, pressures, state, impacts, and responses, totaling 5 levels and 22 specific indicators, of which 11 indicators were natural factors and 11 indicators were anthropogenic factors (see Table II for details). The selection of these 22 indicators is based on the existing literature, as detailed in Supplemental files Table S1.

2) Combined Weighting Method to Determine Indicator Weights: The analytic hierarchy process (AHP) is a typical example of a subjective weighting method, widely used for determining weights due to its convenience and efficiency, allowing for both qualitative and quantitative analysis of indicators; however, its weighting relies on expert scoring [49]. The entropy weight method (EWM) is characteristic of objective weighting approaches, accurately representing indicator weights; although a limitation of objective weighting methods is their exclusive reliance on empirical data for weight determination, unable to adequately consider the decision-makers' professional expertise and knowledge. An integrated weighting method introduces

TABLE II
22 INDICATORS AND THEIR WEIGHTS

Target layer	Guideline layer	Indicator layer	AHP	EWM	Combined weighting
EHI	Driving force (D)	X_{D1} population density	0.03	0.00	0.01
		X_{D2} average annual rainfall	0.08	0.10	0.09
		X_{D3} average annual temperature	0.05	0.02	0.04
	Pressure (P)	X_{P1} amount of tourism revenue	0.01	0.03	0.02
		X_{P2} livestock number	0.04	0.02	0.03
		X_{P3} electricity consumed by residents	0.02	0.02	0.02
		X_{P4} nighttime light	0.01	0.01	0.01
		X_{P5} primary industry	0.05	0.01	0.03
	State (S)	X_{S1} biomass	0.14	0.10	0.12
		X_{S2} vegetation cover	0.13	0.14	0.14
		X_{S3} total evapotranspiration	0.07	0.05	0.06
		X_{S4} soil carbon content	0.04	0.11	0.07
		X_{S5} soil pH	0.03	0.01	0.01
		X_{S6} Soil nutrient availability	0.02	0.10	0.05
		X_{S7} slope	0.02	0.02	0.03
		X_{S8} slope direction	0.03	0.03	0.04
		X_{S9} altitude	0.03	0.01	0.02
	Impact (I)	X_{I1} per capita disposable income	0.05	0.05	0.05
		X_{I2} level of grain production	0.02	0.02	0.02
	Response (R)	X_{R1} area of soil and water erosion control	0.02	0.06	0.04
		X_{R2} number of schoolchildren	0.05	0.05	0.05
		X_{R3} total value of the tertiary industry	0.06	0.04	0.05

the principle of minimum relative entropy, combining the AHP and EWM, thus enhancing the credibility of the evaluation. Its calculation formula is given as follows:

$$W_i = \frac{\sqrt{(W_{1i} \times W_{2i})}}{\sum \sqrt{(W_{1i} \times W_{2i})}} \qquad (1)$$

where W_i represents the aggregate weight of the indicator, encompassing both W_{1i}, the subjective component of the indicator's weight, and W_{2i}, its objective counterpart.

3) TOPSIS Model: The basic principle of the TOPSIS-based integrated assessment model lies in calculating the distance between the assessed objects and the ideal solution and then ranking the assessed objects based on this distance [50]. According to this principle, objects may be deemed ideal only if they are proximate to the positive ideal plan and distant from the negative ideal plan. However, as the condition of ecosystems is influenced by a range of nonlinear ecological factors, traditional simple weighting methods will not only lead to the loss of information

but can also result in misleading ecosystem health assessment outcomes. TOPSIS-based integrated assessment model not only overcomes the aforementioned shortcomings but also has no strict data limitations and has been widely applied to various fields (e.g., renewable energy [51] and risk assessment [52]). The current TOPSIS models are complex, so a combined weighting approach was incorporated to simplify the TOPSIS model and, thus, construct a more rational model. The TOPSIS model is calculated as follows.

Step 1: Normalization of the original value of the indicator to create a normalization matrix. Due to the different sources of initial data, its standardization can eliminate the influence of different dimensions between the indicators so that the value of each indicator within a certain range of uniformity of the evaluation indicators using the minimum value type, the maximum value type, the interval value type, and the middle value type of the normalization method standardizes the evaluation indicators.

Maximum value type indicators ($J1$)

$$T_{ij} = \frac{X_i - \min(X_i)}{\max(X_i) - \min(X_i)}. \tag{2}$$

Minimum value type indicators ($J2$)

$$T_{ij} = \frac{\max(X_i) - X_i}{\max(X_i) - \min(X_i)}. \tag{3}$$

Interval-type indicators ($J3$)

$$T_{ij} = \begin{cases} 1 - \frac{a - X_i}{M}, X_i < a \\ 1, a \le X_i \le b, \quad M \\ 1 - \frac{X_i - b}{M}, X_i > b. \end{cases}$$
$$= \max\{a - \min\{X_i\}, \max\{X_i\} - b\} \tag{4}$$

Intermediate indicators ($J4$)

$$T_{ij} = 1 - \frac{|X_i - X_{\text{best}}|}{M}, \quad M = \max\{|X_i - X_{\text{best}}|\}. \tag{5}$$

Step 2: Assuming that there are n objects to be evaluated and m evaluation indicators, the composition matrix is shown as follows:

$$T = \begin{bmatrix} T_{11} & T_{12} & \cdots & T_{1m} \\ T_{21} & T_{22} & \cdots & T_{2m} \\ \vdots & \vdots & \cdots & \vdots \\ T_{n1} & T_{n2} & \cdots & T_{nm} \end{bmatrix}. \tag{6}$$

Step 3: Calculate the product of the standardized decision matrix and the weight vector, and then the weighted standardized decision matrix was established

$$U_{ij} = W_i \times T_{ij} \tag{7}$$

$$U = \begin{bmatrix} U_{11} & U_{12} & \cdots & U_{1m} \\ U_{21} & U_{22} & \cdots & U_{2m} \\ \vdots & \vdots & \cdots & \vdots \\ U_{n1} & U_{n2} & \cdots & U_{nm} \end{bmatrix}. \tag{8}$$

Step 4: According to the weighted standardized decision matrix, the ideal solution and the negative ideal solution were obtained, and the distance of the evaluation object to the understanding and ideal solution was calculated

$$\begin{cases} U_i^+ = \{U_1^+, U_2^+, \ldots, U_n^+\} \\ \quad = \{(\max U_{ij}, j \in J_1), (\min U_{ij}, j \in J_2)\} \\ U_i^- = \{U_1^-, U_2^-, \ldots, U_n^-\} \\ \quad = \{(\min U_{ij}, j \in J_1), (\max U_{ij}, j \in J_2)\} \end{cases}. \tag{9}$$

Step 5: Distance of the ith ($i = 1,2,\ldots,n$) evaluation object from the maximal value

$$D_i^+ = \sqrt{\sum_{j=1}^m (U_j^+ - U_{ij})^2}. \tag{10}$$

Step 6: Distance of the ith ($i = 1,2,\ldots,n$) evaluation object from the minimum

$$D_i^- = \sqrt{\sum_{j=1}^m (U_j^- - U_{ij})^2}. \tag{11}$$

TABLE III
ECOSYSTEM HEALTH LEVELING

level	EHI range	ecosystem health level
Level 1	min–0.299	Weak
Level 2	0.299–0.349	Relatively weak
Level 3	0.349–0.397	Ordinary
Level 4	0.397–0.518	Relatively well
Level 5	0.518–max	Well

Step 7: Finally, the distance between the object and the ideal solution was calculated according to the following equation:

$$C_i = \frac{D_i^-}{D_i^+ + D_i^-} (0 \le C_i \le 1) \tag{12}$$

$$\text{EHI} = C_i. \tag{13}$$

By applying the TOPSIS assessment model to overlay and analyze the indicators, the article obtains a composite ecosystem health index (EHI) for every single period. The natural discontinuity classification method was adopted, and the study area was combined to categorize the EHI into the following levels: weak, relatively weak, ordinary, relatively well, and well. The specific grading ranges are shown in Table III.

4) Ecosystem Health Trend Analysis: To ascertain the spatiotemporal patterns of EHI variations spanning the years 2000–2020, a linear regression analysis methodology was employed. The equation is given as follows:

$$\text{slop} = \frac{n \times \sum_{i=1}^n i \times \text{EHI}_i - \sum_{i=1}^n i \sum_{i=1}^n \text{EHI}_i}{n \times \sum_{i=1}^n i^2 - \left(\sum_{i=1}^n i\right)^2}. \tag{14}$$

In this context, "slope" refers to the gradient of the EHI trendline. A slope greater than zero indicates an ascending trend in the EHI, whereas a slope less than zero signifies a descending trend. To further investigate the changes in the spatial distribution of Xinjiang's EHI, the results were categorized as severe deterioration (slope ≤ -0.002), slight deterioration ($-0.002 <$ slope ≤ -0.0001), steady ($-0.0001 <$ slope ≤ 0.0001), slight improvement ($0.0001 <$ slope ≤ 0.002), and obvious improvement (slope > 0.002).

5) Spatial Autocorrelation Analysis: Spatial autocorrelation was performed using Moran's I scatter plots and local indicators of spatial association aggregation plots to assess the degree of spatial aggregation of similar and dissimilar samples [9]. Moran's I coefficients were used to reflect the degree of localized spatial autocorrelation. The formula can be articulated as follows:

$$\text{Moran'I} = \frac{\sum_{i=1}^n \sum_{j\ne i}^n W_{ij} (X_i - \bar{X})(X_j - \bar{X})}{S^2 \sum_{i=1}^n \sum_{j\ne i}^n W_{ij}} \tag{15}$$

$$\text{Local Moran'I} = \frac{n(x_i - \bar{x}) \sum_{j=1}^m w_{ij}(x_j - \bar{x})}{\sum_{i=1}^n (x_i - \bar{x})^2} \tag{16}$$

$$S^2 = \frac{1}{n} \sum_{i=1}^n (X_i - \bar{X})^2 \tag{17}$$

$$Z = \frac{1 - E(I)}{\sqrt{\mathrm{VAR}(I)}}. \tag{18}$$

In the aforementioned context, n represents the total count of samples, while W_{ij} denotes the matrix of spatial weights, Moran's I > 0 indicates that the EHI displays aggregation, Moran's I < 0 indicates that the EHI is dispersed, Moran's I $= 0$ indicates a spatially random distribution of the EHI, $E(I)$ and $\mathrm{VAR}(I)$ are the expectation and variance in Moran's index, and $Z > 2.58$ or $Z < -2.58$ indicates that spatial autocorrelation is significant, as evidenced by the 99% confidence level.

6) Geographical Detector: Compared with traditional PCA [18] and regression analysis methods, the geodetector model has been proven effective in understanding the spatial heterogeneity of geographic phenomena and variations among these driving factors. The geodetector model delves into the exploration of influential factors and their interplay, focusing on both the detection of these factors and the examination of their interactions [53]. Factor detection measures the influence of influencing factors on the EHI; as the value of factor detection (q) increases, so does the impact of various influencing factors on the EHI

$$q = 1 - \frac{\sum_h^L N_h \sigma_h^2}{N\sigma^2} \tag{19}$$

where $h = 1, \ldots, L$ represents the count of divisions within the study area segmented according to each influencing factor in each partition h, N_h denotes the number of grids, the study area comprises a total of N grids, σ_h^2 is the variance in the EHI in partition h, and σ^2 is the total variance in the EHI in the study area. The obtained q-values range from 0 to 1.

Interaction detection involves the effect of interactions between any two factors on EHI changes, ascertaining whether these influencing factors operate independently or in conjunction. The approach initially determines the extent of the impact value for each of the two X factors independently, $q(X1)$ and $q(X2)$; subsequently, it computes the q-value during their interaction: $(q(X1 \cap X2))$.

7) OLS and GWR Model: While the geodetector model cannot offer spatial representations of variable correlations, the GWR model addresses this shortcoming effectively by assessing the spatial variability of influencing factors. In this study, ordinary least square (OLS) and GWR methodologies were employed to examine the underlying mechanisms influencing the EHI. First, OLS methodology was applied to explore the linear correlation between the EHI and its influencing factors. The regression model was defined in the following manner:

$$y_i = \beta_0 + \sum \beta_j x_i + e_i. \tag{20}$$

Here, y_i is the EHI for the ith grid, and x_i is the selected factor for the ith grid. β_0 represents the coefficient of the constant term, β_j denotes the coefficient of the explanatory variable, and e_i is identified as the stochastic error term.

GWR models are capable of identifying spatially nonstationary interactions between independent and dependent variables [54]. These methods are also employed in assessing the spatial variability of climate change and human-induced alterations in ecosystem health. The GWR model, a localized

spatial regression approach, leverages spatial relationships at various sampling points. It elucidates the connection between independent and dependent variables in relation to their spatial positioning, thereby uncovering overlooked local spatial dynamics [55]. Prior to implementing the GWR model, an OLS model analysis was conducted to identify potential multicollinearity among variables utilizing the variance inflation factor (VIF) as a diagnostic tool, and the variables were judged to be significant based on the b value. The GWR model was expressed as follows:

$$y_l = \beta_o(u_l, v_l) + \sum_{k=1}^{p} \beta_k(u_l, v_l)x_{lk} + \varepsilon_l \tag{21}$$

where y_l denotes the EHI; x_{lk} represents the dependent variable and the kth independent variable at location l; u_l and v_l indicate the geographic coordinates of location l; p represents the count of independent variables at location l; and $\beta_k(u_l, v_l)$ signifies the local regression coefficient for the jth explanatory variable. This coefficient indicates the extent of impact that the independent variable has on the dependent variable, where greater absolute values of the coefficient imply a more substantial influence, $\beta_o(u_l, v_l)$ represents the intercept corresponding to location l, and ε_l represents the term for random noise.

8) Hurst Exponent and R/S Analysis: The Hurst exponent is useful for understanding the properties of a time series without making assumptions about statistical restrictions. It also takes into account the effects of multiple influencing factors within ecosystems, thus providing a more comprehensive health assessment. R/S analysis, commonly referred to as rescaled range analysis, is extensively utilized for determining the Hurst exponent [56]. The results can be categorized as follows.

1) $0 < \text{Hurst} < 0.5$ indicates that the time series is antipersistent, showing that the series has a counter trend in the future.
2) $\text{Hurst} = 0.5$ indicates that the time series is uncertain.
3) $0.5 < \text{Hurst} < 1$ implies the persistence of the series, which suggests that the trend identified in the analysis period is likely to persist moving forward.

In this study, by combining the Hurst exponent with slope trend analysis from 2000 to 2020, the possible future trends of the EHI after 2020 can be defined as follows:

1) increase and persistence (slope > 0, $0.5 < \text{hurst} < 1$);
2) decrease and persistence (slope < 0, $0.5 < \text{hurst} < 1$);
3) decrease and antipersistence (slope < 0, $0 < \text{hurst} < 0.5$);
4) increase and antipersistence (slope > 0, $0 < \text{hurst} < 0.5$).

The calculation equations of the Hurst exponent (R/S analysis) are given as follows:

$$\bar{M}_\tau = \frac{1}{\tau}\sum_{t=1}^{\tau} M_{(t)}, t = 1, 2, \ldots, n \tag{22}$$

$$X(t, \tau) = \sum_{1}^{\tau}(M_{(t)} - \bar{M}_{(t)}), 1 \le t \le \tau \tag{23}$$

$$R_\tau = \max_{1 \le t \le \tau} X_{(t,\tau)} - \min_{1 \le t \le \tau} X_{(t,\tau)} \tag{24}$$

$$S_{(\tau)} = \sqrt{\frac{1}{\tau}\sum_{t}^{\tau}\left(M_{(t)} - \bar{M}_{(\tau)}\right)^2} \tag{25}$$
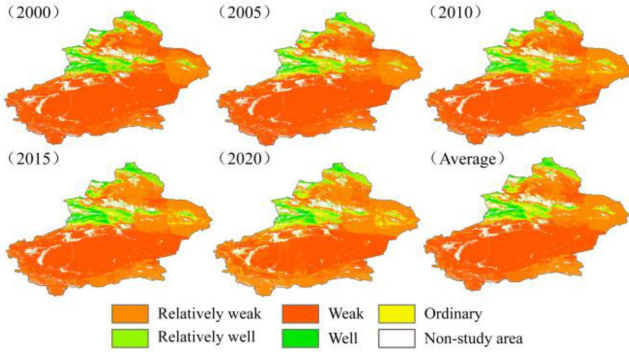
Fig. 2.   Geographical patterns of ecosystem health levels from 2000 to 2020.

$$\log\left(R/S\right)_\tau = c + H \times \log(\tau) \qquad (26)$$

where $X(t, \tau)$ is the cumulative deviation, $R(\tau)$ is the extreme deviation, $S(\tau)$ is the standard deviation, C is a constant, and H is the Hurst exponent.

III. RESULTS

A. Characteristics of Spatial Patterns and Spatiotemporal Changes in the EHI

1) Spatial Pattern of the EHIs: As shown in Fig. 2, the ecosystem health levels in most regions of Xinjiang during the period 2000–2020 were between weak and relatively weak. Ecosystem health levels exhibited a spatial pattern, being more robust in northern regions but lower in southern regions, with high-level areas occurring mainly in the Altai Mountains and Tian Shan Mountains and northeast and low-level areas occurring mainly in the Junggar Basin and Tarim Basin regions. Notably, the ecosystem health levels near the Junggar Basin and the Kunlun Mountains gradually increased over time, with the health level in eastern Xinjiang slightly increasing in 2010 compared with that in 2005 but returning to the 2005 health level in 2015; moreover, there were no significant changes in the health level in other regions.

2) Characteristics of Spatial and Temporal Changes in the EHI: From 2000 to 2020, there was a marked increase in the Xinjiang EHI, with the regions showing improvement comprising 92.1% of the total area under study (see Fig. 3). The deteriorated areas were mainly located in the western part of the Altai Mountains and Tian Shan Mountains and the central part of the study area, and their share was only 4.4%. Regions exhibiting stable conditions constituted 3.5% of the overall area. The EHI of the southwestern and eastern parts of Tian Shan significantly improved.

To understand the changes between different levels in Xinjiang Province between 2000 and 2020, the study period was divided into four phases. Fig. 4 shows that the proportion of area graded as weak continued to decrease, from 61.39% in 2000 to 37.44% in 2020. The proportion of weak graded areas decreased the most from 2005 to 2010, with a total decrease of 9.71% in these five years. The proportion of acreage classified as relatively weak continued to increase over the study period,
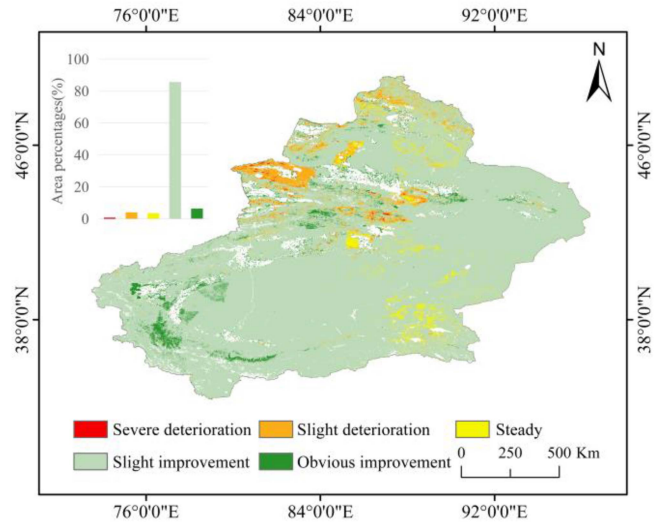

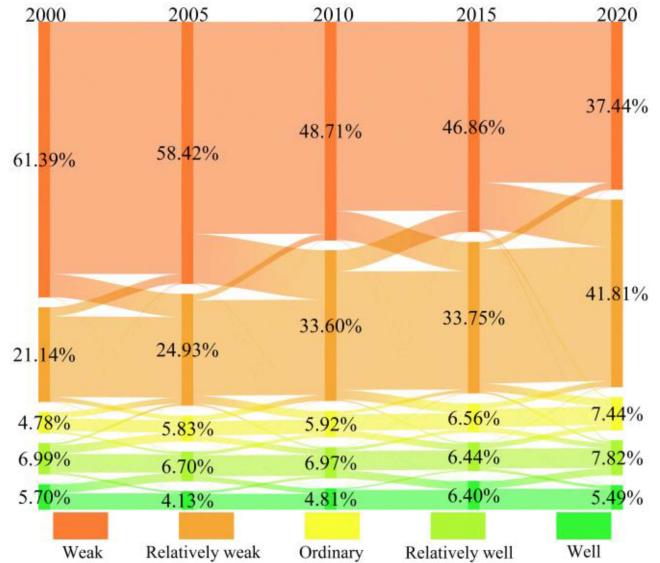Fig. 3.   Extent of change in the EHIs in Xinjiang, 2000–2020.

Fig. 4.   Shifts in ecosystem health levels from 2000 to 2020.

with increases of 3.79%, 8.67%, 0.15%, and 8.06% for each of the four phases. From 2000 to 2020, the alterations in ecosystem health were marked by a reduction in the percentage of areas with a weak level, a rise in the percentage of areas with a relatively weak level, and a negligible shift in the percentage of areas with other levels.

B. Ecosystem Health Center of Gravity Shift and Spatial Analysis

1) Center of Gravity Shift of Different Health Classes: The center of gravity model was employed to ascertain the coordinates that represent the center of gravity across different ecosystem health levels; the spatial migration is shown in Fig. 5. The spatial distribution pattern of "weak" → "relatively weak" → "ordinary" → "relatively well" → "well" occurred from south
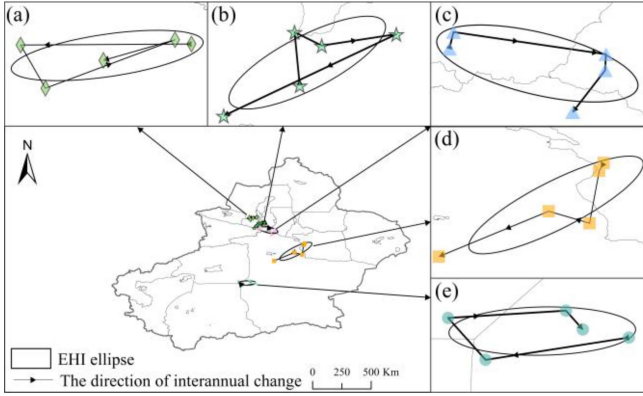
Fig. 5. Spatial migration of the center of gravity of each ecosystem health level in Xinjiang from 2000 to 2020. Note: *a, b, c, d,* and *e* represent the centers of gravity of the well, relatively well, ordinary, relatively weak, and weak, respectively.
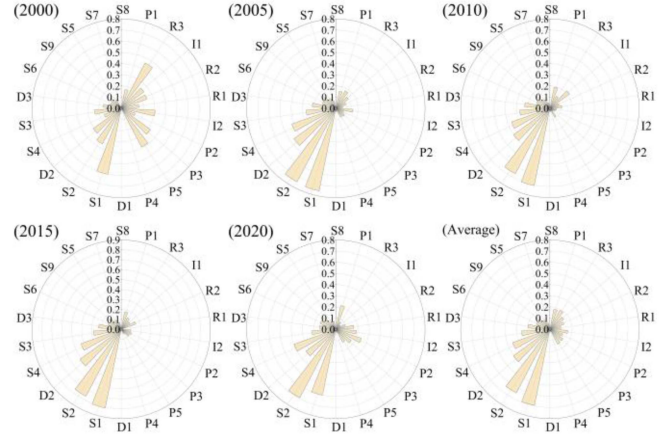

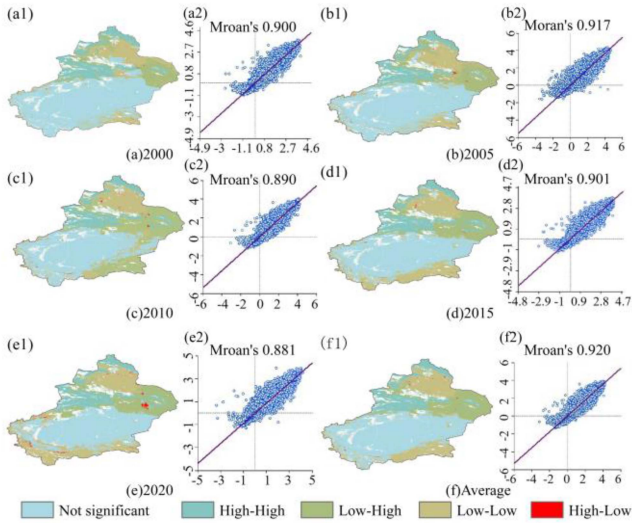Fig. 7. Detection results of each index factor.

Fig. 6. Spatial autocorrelations of the EHI for 2000–2020 and 21-year averages, including Moran's I scatterplots of the EHI (*a*1, *b*1, *c*1, *d*1, *e*1, and *f*1) and localized spatial autocorrelations of the EHI (*a*2, *b*2, *c*2, *d*2, *e*2, and *f*2).

to northeast and then to northwest in the study area, indicating serious ecological health problems in the study area's southern region. The center of gravity for the ecosystem's relatively weak level progressively shifted southwestward over time. The center of gravity of the ordinary level first moved to the southeast and then to the southwest, while the center of gravity of the other levels tended to form a closed loop; the spatial distribution of the centers of gravity of the different health classes had an elliptical shape.

2) Spatial Autocorrelation Analysis: The spatial correlation of the EHI in the designated study area was verified using Moran's I scatter plot and global spatial autocorrelation analysis. Fig. 6 shows that the global Moran's I > 0 indicates a strong positive spatial correlation of the EHI in the study area. The local spatial correlation among the EHI was further analyzed, and a map of the local spatial autocorrelation agglomeration was obtained. The main type of spatial clustering in the study area,

which was labeled "not significant," as shown in Fig. 6, predominantly occurred in the Tarim Basin. In contrast, the "Low–Low" classification was primarily observed in the Junggar Basin. The least common type was "High–Low", which was sporadically distributed in the northern and eastern parts of the country.

C. Analysis of Driving Factors

1) Geodetector Factor Detection: The q-values of different driving factors gradually change over time. As shown in Fig. 7, in terms of the average, the impact strengths of factors biomass ($S1$) reached a q-value of 0.72, which was the highest value, followed by vegetation cover ($S2$); the q-values for these two factors significantly exceeded those of the remaining factors. The average annual rainfall ($D2$), soil carbon content ($S4$), total evapotranspiration ($S3$), and average annual temperature ($D3$) followed; these factors are all natural factors. For the anthropogenic factors, the first- and second-ranked factors were tourism revenue ($P1$) and tertiary gross output value ($R3$), with q-values of 0.17 and 0.15, respectively. The lowest ranked factor was slope direction, with a q-value of 0.05, while the q-values for the remaining factors varied, falling within a range of 0.1–0.2, indicating that their impact on the EHI was comparatively minor.

2) GWR Model: In accordance with the outcomes from the OLS regression, factors exhibiting VIF values exceeding 7.5 and b values surpassing 0.01 were omitted from consideration. The remaining factors were combined with the ranking of the geodetector q-value results. Finally, four natural factors, $S1$ (biomass), $S2$ (vegetation cover), $S3$ (total evapotranspiration), and $D2$ (average annual rainfall), and two anthropogenic factors, $I1$ (per capita disposable income) and $R3$ (total tertiary industry value), were selected as the dominant driving factors. The outcome of the OLS analysis, applied to the dominant driving factors, indicated a significant Koenker value. Consequently, these selected factors were incorporated as inputs in the GWR model; the model-adjusted $R^2 = 0.87$ and the model residuals of Moran I = 0.6 and $z = 509$, proving a good model fit. The results after superposition of the maximum driving factor are $S1$ (biomass), which was mainly located near the Altai and
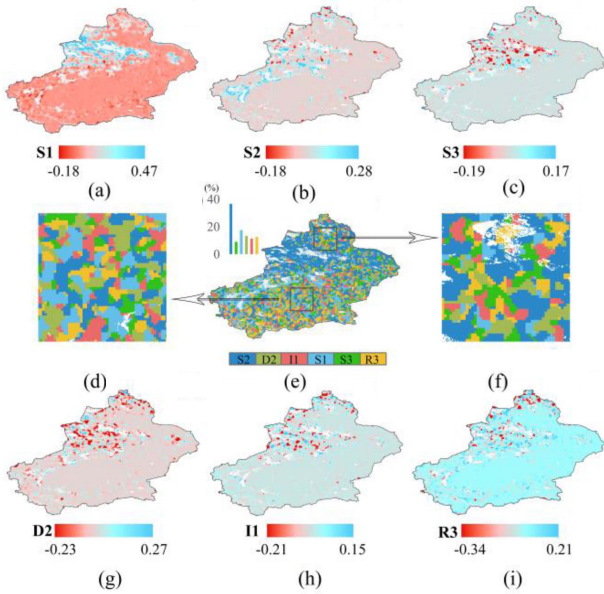
Fig. 8. Spatial distribution of dominant driving factors and spatial variability of regression coefficients. Notes: *a, b, c, g, h*, and *i* represent the spatial variability coefficients of each dominant driver. *e*: The spatial distribution of the dominant drivers and their percentage of area.

Fig. 9. Dominant driver interaction detection results. Note: "∗" indicates the nonlinear enhancement, and the rest denotes the bienhancement.
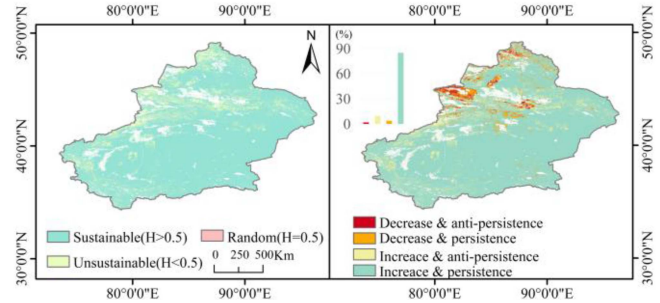

Fig. 10. Spatial Hurst (H) index (left). EHI projected trends and percentage of area occupied by each trend (right).

Tian Shan mountain ranges. The largest driver, $S2$ (vegetation cover), was mainly located in the southwestern part of the study area, and the remaining four factors were dominant in similar areas, mainly concentrated in areas bordering the south. Fig. 8 shows the results of the regression analyses of the dominant driving factors on the EHI. In general, each factor had both positive and negative influences. Similarly, the coefficients $D2$ (mean annual rainfall) and $S3$ (total evapotranspiration) were distributed, with the lowest and highest values occurring near the Altai Mountains and Tian Shan, whereas the coefficients of all the factors occurring near the Junggar Basin and the Tarim Basin were nearly zero. The highest coefficients of $S2$ (vegetative cover) were mainly concentrated in the northwestern corner of the Tarim Basin, while the negative values were mainly distributed in the Altai Mountains, Tian Shan Mountains, and southern part of the Tarim Basin. The highest values of the coefficients of $S1$ (biomass) were mainly distributed near the Tian Shan Mountains, while the negative values were mainly distributed in the western part of the Tarim Basin.

3) Interaction Detection: The findings from the interaction detection analysis, as illustrated in Fig. 9, demonstrated that there were two types of interactions between factors, namely, bienhancement and nonlinear enhancement. The enhancement observed in the nonlinear enhanced domain led to a markedly greater interaction effect of the two factors when compared with the impact exerted by any single factor independently. During the study period, the combined effect of any two factors exceeded the individual impact of any one factor on the EHI, indicating the interdependence of the drivers. Specifically, most of the interactions among $S1$ (biomass), $S2$ (vegetation cover), $S3$ (total evapotranspiration), and $D2$ (average annual rainfall) and other factors were bienhanced; thus, these four factors were

the primary drivers of the alterations. While the interactions between $I1$ (per capita disposable income) and $R3$ (total value of tertiary industry) and other factors showed more of a nonlinear enhancement, their combination with other factors still showed a strong influence.

D. Possible Future Trends in the EHI

Fig. 10 indicates that regions exhibiting an increase and persistent trend in the EHI encompassed 85.05% of the total area analyzed, with these areas extending across almost the entire region being studied, while the regions exhibiting an increase and antipersistent trend in the EHI constituted 9.47% of the overall area studied. Primarily, these regions were located in the central and eastern sections of the Tian Shan Mountains, as well as along the periphery of the Tarim Basin. Furthermore, 3.70% of the regions exhibited a decrease and persistent trend in the EHI; most of these areas were situated in the western part of the Tian Shan Mountains, and only 1.78% showed a decrease and antipersistent trend. These areas were sporadically distributed in the western and central parts of the Tian Shan Mountains and near the Altai Mountains; no area exhibited an uncertain trend in this study.

IV. DISCUSSION

A. Comparison of Results by Previous Studies

At present, there are only few ecosystem health assessments of the entire Xinjiang region, so related research results are used for validation. Li et al. [41] evaluated the ecosystem health in southern Xinjiang and reported generally low health levels. He et al. [9], who conducted a county-level national ecosystem health assessment, noted an increasing gradient of ecosystem health from south to north in Xinjiang. Study on the ecosystem health in Central Asia by Yushanjiang et al. [57] shows that the ecosystems near the Altai and Tian Shan Mountains are in better conditions, while those in the Junggar and Tarim Basins are less healthy. These results largely align with the DPSIR-TOPSIS model's result, thus further validating the results of this model.

B. Characteristics of Temporal and Spatial Changes in Ecosystem Health

Regarding the temporal changes in ecosystem health (see Fig. 4), the EHI in Xinjiang has gradually improved since 2000 for two main reasons. First, a variety of measures for ecological conservation and environmental safeguarding have been implemented in Xinjiang Province, including returning farmland to forests, the 10th Five-Year Plan and 11th Five-Year Plan, and strengthened ecological and environmental protection [34], which have strongly contributed to the improvement of ecosystem health. Second, in recent years, a warmer and wetter climate pattern has gradually developed in Xinjiang [58]. Higher temperatures accelerated the melting of glaciers in high mountains [59], and these factors contributed to the enhancement of vegetation growth in the region [60]. Research indicates that plants play a pivotal role in maintaining the health of ecosystems, and improvements in vegetation can enhance the health of ecosystems. Regarding the spatial distribution of ecosystem health, certain areas exhibited significant ecological difficulties (see Fig. 3). Areas exhibiting greater EHIs were predominantly located adjacent to the Altai and Tian Shan Mountains' ranges and were characterized by a landscape largely composed of forests and grasslands; these areas were noted for their significant net primary productivity; additionally, their biomass ($S1$) and vegetation cover ($S2$) indices were high. Thus, their ecosystems had better health. The regions with lower EHI were located in the Junggar Basin and the Tarim Basin, which face serious problems related to water evaporation and poor soil quality. Compared with those in the Tarim Basin, the Junggar Basin had a greater EHI; however, although the average rainfall in both regions was less than 300 mm/a, the Junggar Basin had relatively high precipitation [58], and its surface productivity responded positively to the increase in the rate of precipitation change, which is more favorable for vegetation growth and, thus, improved ecosystem health.

C. Driving Factor Analysis and Its Impact on Ecological Conservation

Identifying the key factors that influence ecosystem health is vital not only for advancing scientific inquiry but also for informing policy decisions and practical applications [52]. The outcomes from the geodetector model revealed that the q-values of biomass ($S1$) and vegetation cover ($S2$) were high, and these two factors as the strongest influencing factors accounted for half of the whole study area; therefore, the Xinjiang region should strengthen the transformation of its economic development and implement additional ecological conservation projects, such as planting plants with high cold and drought resistance; this approach has the potential to greatly enhance plant growth and mitigate soil degradation and aid in the recovery of natural habitats [61], [62]. However, the GWR modeling results showed that all the dominant drivers had dual impacts on ecosystem health, exhibiting both positive and negative effects. This complexity highlights that ecosystem health is multifactorial and multidimensional and influenced by spatial variability in geographic and ecological environments. This study showed that unused land has the lowest level of ecosystem health, forest ecosystem health is the highest, grassland ecosystem health is in between these two levels, and unused land is more difficult to restore due to severe water scarcity and poor natural conditions. Therefore, with limited resources, enhancing the ecological quality of grasslands should be considered a top priority. The following measures can be taken: adopt rotational grazing and cyclic closure practices for grasslands; and control livestock quality and introduce breeds that have less impact on the grassland ecological environment. In addition, Fig. 10 indicates that ecosystem health in most areas will improve in the future; however, this trend does not mean that ecosystems in most areas of Xinjiang will remain healthy in the future; moreover, the ecological health problems in Xinjiang will still be serious. It is important to strengthen ecological reconstruction, control pollution sources, and develop environmentally friendly tertiary industries to continue to reduce the degree of ecological environmental damage caused by human development.

D. Limitations and Future Research Directions

The results indicate that the impacts of different indicators on ecosystem health are not isolated but interrelated. But the DPSIR model assumes that each indicator is independent and arranges them in the order of pressure, state, impact, and response, which may affect its accuracy. Second, when forecasting future ecosystem health, the Hurst exponent focuses only on numerical patterns and does not adequately consider the influence of external factors, such as changes in policy, which may significantly impact ecosystem health. Finally, the results of this study still require further validation. Future research needs to focus more on the validation part. Multiple methodologies and data may be required for comprehensive validation to confirm the reliability and scientific integrity of the results. Furthermore, previous research has indicated that in areas sensitive to ecological changes, climate significantly impacts the health of ecosystems [63]; however, in this study, climatic factors did not emerge as the dominant driver. This finding may be due to the selection of the average annual temperature, for which temperature variations are relatively insignificant. In contrast, Xinjiang's climate is marked by substantial temperature fluctuations between day and night, along with regular occurrences of extreme weather

conditions [64]. Therefore, it is important for future research to focus more on how extreme weather events impact the health of ecosystems. In this study, the DPSIR-TOPSIS model was used to assess ecosystem health in the Xinjiang region. Given the intricate relationship between natural ecosystems and socioeconomic systems, the ecosystem health assessment framework and its drivers need to be further investigated [65].

Despite some limitations, the methods used in this study still have considerable value. Compared with the traditional comprehensive weighted assessment approach, the DPSIR-TOPSIS model can be used to assess ecosystem health effectively and in depth in Xinjiang. The application of the geodetector model and GWR model not only analyzes the relative importance of the driving factors but also explores the degree of spatial variability of each factor and reveals the interactions among these factors. The combination of the Hurst exponent and slope trend analysis revealed the future trend of ecosystem health. This research provides an analysis of the spatial and temporal variations in ecosystem health, offering valuable perspectives on evolving patterns as well as future projections. This knowledge is crucial for guiding the development of scientific strategies for ecological conservation and restoration efforts in Xinjiang.

V. CONCLUSION

In this article, the DPSIR-TOPSIS model was constructed to comprehensively assess and analyze the spatial and temporal characteristics of ecosystem health in Xinjiang from 2000 to 2020. In addition, the introduction of a geographical detector and a GWR model facilitated the analysis of various factors influencing ecosystem health. Finally, the Hurst exponent, in conjunction with slope trend analysis, was employed to predict future trends in ecosystem health. This approach aims to harmonize regional economic growth with the protection of environmental resources. The key conclusions of this research are outlined as follows.

1) In Xinjiang, the ecosystem health level is greater near the Altai and Tian Shan Mountains but lower in the Junggar and Tarim Basins. Additionally, there was a steady increase in the EHI over the course of the study, revealing a positive spatial correlation.
2) Among the dominant driving factors, natural factors include $S1$ (biomass), $S2$ (vegetation cover), $S3$ (total evapotranspiration), and $D2$ (average annual rainfall), and anthropogenic factors include $I1$ (per capita disposable income) and $R3$ (total value of the tertiary industry). The dominant driving factors in different regions are different, the influencing factors are complex, and enhanced interactions occur between different driving factors.
3) In the future, 86.83% of the areas in Xinjiang will experience an increasing trend in the EHI, and ecosystem health will gradually improve.

REFERENCES

[1] N. H. Pan, Q. Q. Du, Q. Y. Guan, Z. Tan, Y. F. Sun, and Q. Z. Wang, "Ecological security assessment and pattern construction in arid and semi-arid areas: A case study of the Hexi region, NW China," *Ecol. Indicators*, vol. 138, May 2022, Art. no. 108797.

[2] Z. Ouyang et al., "Improvements in ecosystem services from investments in natural capital," *Science*, vol. 352, no. 6292, pp. 1455–1459, Jun. 2016.

[3] S. Wang, Y. Huang, X. Jiang, T. Wang, and Y. Jin, "Identification and optimization of ecological security patterns in the Xiangyang metropolitan area," *IEEE J. Sel. Topics Appl. Earth Observ. Remote Sens.*, vol. 16, pp. 8671–8679, Aug. 2023.

[4] H. R. Cheng, L. K. Zhu, and J. J. Meng, "Fuzzy evaluation of the ecological security of land resources in mainland China based on the pressure-state-response framework," *Sci. Total Environ.*, vol. 804, Jan. 2022, Art. no. 150053.

[5] M. M. Ding et al., "Construction and optimization strategy of ecological security pattern in a rapidly urbanizing region: A case study in central-south China," *Ecol. Indicators*, vol. 136, Mar. 2022, Art. no. 108604.

[6] Q. Li, Y. Zhou, and S. Q. Yi, "An integrated approach to constructing ecological security patterns and identifying ecological restoration and protection areas: A case study of Jingmen, China," *Ecol. Indicators*, vol. 137, Apr. 2022, Art. no. 108723.

[7] Y. T. Wang, Y. S. Wang, M. L. Wu, C. C. Sun, and J. D. Gu, "Assessing ecological health of mangrove ecosystems along South China Coast by the pressure-state-response (PSR) model," *Ecotoxicology*, vol. 30, no. 4, pp. 622–631, May 2021.

[8] J. J. Lei, C. S. Li, and W. N. Yang, "Ecosystem health assessment and approaches to improve Sichuan Province based on an improved vigor organization resilience model," *Ecol. Indicators*, vol. 155, Nov. 2023, Art. no. 110925.

[9] J. H. He, Z. Z. Pan, D. F. Liu, and X. N. Guo, "Exploring the regional differences of ecosystem health and its driving factors in China," *Sci. Total Environ.*, vol. 673, pp. 553–564, Jul. 2019.

[10] J. Peng, Y. X. Liu, J. S. Wu, H. L. Lv, and X. X. Hu, "Linking ecosystem services and landscape patterns to assess urban ecosystem health: A case study in Shenzhen City, China," *Landscape Urban Plan.*, vol. 143, pp. 56–68, Nov. 2015.

[11] Z. H. Dong, J. Q. Zhang, Z. J. Tong, A. R. Han, and F. Zhi, "Ecological security assessment of Xilingol grassland in China using DPSIRM model," *Ecol. Indicators*, vol. 143, Oct. 2022, Art. no. 109336.

[12] B. Yang, L. J. Ding, X. Y. Zhan, X. Z. Tao, and F. Peng, "Evaluation and analysis of energy security in China based on the DPSIR model," *Energy Rep.*, vol. 8, pp. 607–615, Jul. 2022.

[13] Y. J. Wang, M. Zhang, C. G. Yang, Y. He, and M. T. Ju, "Regional water pollution management pathways and effects under strengthened policy constraints: The case of Tianjin, China," *Environ. Sci. Pollut. Res.*, vol. 29, no. 51, pp. 77026–77046, Nov. 2022.

[14] D. A. Mariano et al., "Use of remote sensing indicators to assess effects of drought and human-induced land degradation on ecosystem health in Northeastern Brazil," *Remote Sens. Environ.*, vol. 213, pp. 129–143, Aug. 2018.

[15] M. Hernández-Blanco et al., "Ecosystem health, ecosystem services, and the well-being of humans and the rest of nature," *Glob. Change Biol.*, vol. 28, no. 17, pp. 5027–5040, Sep. 2022.

[16] J. Li and W. Shen, "Spatial heterogeneity of the effects of human activities on ecosystem health of a coastal tourism city—A case study of Rizhao, China," *Appl. Ecol. Environ. Res.*, vol. 19, no. 4, pp. 3029–3051, 2021.

[17] W. J. Li, S. Y. Xie, Y. Wang, J. Huang, and X. Cheng, "Effects of urban expansion on ecosystem health in Southwest China from a multi-perspective analysis," *J. Cleaner Prod.*, vol. 294, Apr. 2021, Art. no. 126341.

[18] Q. H. Yuan et al., "Ecosystem health of the Beiyun River basin (Beijing, China) as evaluated by the method of combination of AHP and PCA," *Environ. Sci. Pollut. Res.*, vol. 29, no. 26, pp. 39116–39130, Jun. 2022.

[19] L. Y. Yang, W. X. Chen, S. P. Pan, J. Zeng, Y. H. Y. Yuan, and T. C. Gu, "Spatial relationship between land urbanization and ecosystem health in the Yangtze River Basin, China," *Environ. Monit. Assessment*, vol. 195, no. 8, Aug. 2023, Art. no. 957.

[20] L. Na, Y. Shi, and L. Guo, "Quantifying the spatial nonstationary response of influencing factors on ecosystem health based on the geographical weighted regression (GWR) model: An example in Inner Mongolia, China, from 1995 to 2020," *Environ. Sci. Pollut. Res.*, vol. 30, no. 29, pp. 73469–73484, Jun. 2023.

[21] S. M. Jiang, F. Feng, X. N. Zhang, C. Y. Xu, B. Q. Jia, and R. Lafortezza, "Ecological transformation is the key to improve ecosystem health for resource-exhausted cities: A case study in China based on future development scenarios," *Sci. Total Environ.*, vol. 921, Apr. 2024, Art. no. 171147.

[22] R. Xiao, Y. X. Guo, Z. H. Zhang, and Y. S. Li, "A hidden Markov model based unscented Kalman filtering framework for ecosystem health prediction: A case study in Shanghai-Hangzhou bay urban agglomeration," *Ecol. Indicators*, vol. 138, May 2022, Art. no. 108854.

[23] L. R. Meng, J. Huang, and J. H. Dong, "Assessment of rural ecosystem health and type classification in Jiangsu Province, China," *Sci. Total Environ.*, vol. 615, pp. 1218–1228, Feb. 2018.

[24] M. R. Su and B. D. Fath, "Spatial distribution of urban ecosystem health in Guangzhou, China," *Ecol. Indicators*, vol. 15, no. 1, pp. 122–130, Apr. 2012.

[25] P. Kang, W. P. Chen, Y. Hou, and Y. Z. Li, "Linking ecosystem services and ecosystem health to ecological risk assessment: A case study of the Beijing-Tianjin-Hebei urban agglomeration," *Sci. Total Environ.*, vol. 636, pp. 1442–1454, Sep. 2018.

[26] C. Zeng, X. Z. Deng, S. Xu, Y. T. Wang, and J. X. Cui, "An integrated approach for assessing the urban ecosystem health of megacities in China," *Cities*, vol. 53, pp. 110–119, Apr. 2016.

[27] X. Cheng, L. D. Chen, R. H. Sun, and P. R. Kong, "Land use changes and socio-economic development strongly deteriorate river ecosystem health in one of the largest basins in China," *Sci. Total Environ.*, vol. 616, pp. 376–385, Mar. 2018.

[28] M. Niu, J. Wang, T. Zuo, Y. Li, and Z. Cheng, "Health assessment of coastal fishery waters in the yellow river estuary based on the fish index of biotic integrity," *J. Hydroecol.*, vol. 44, no. 6, pp. 45–52, 2023.

[29] Y. Chi, W. Zheng, H. H. Shi, J. K. Sun, and Z. Y. Fu, "Spatial heterogeneity of estuarine wetland ecosystem health influenced by complex natural and anthropogenic factors," *Sci. Total Environ.*, vol. 634, pp. 1445–1462, Sep. 2018.

[30] D. M. Styers, A. H. Chappelka, L. J. Marzen, and G. L. Somers, "Developing a land-cover classification to select indicators of forest ecosystem health in a rapidly urbanizing landscape," *Landscape Urban Plan.*, vol. 94, no. 3/4, pp. 158–165, Mar. 2010.

[31] J. Q. Yao, Y. N. Chen, X. F. Guan, Y. Zhao, J. Chen, and W. Y. Mao, "Recent climate and hydrological changes in a mountain-basin system in Xinjiang, China," *Earth-Sci. Rev.*, vol. 226, Mar. 2022, Art. no. 103957.

[32] C. C. Xu, Y. N. Chen, Y. H. I. Yang, X. M. Hao, and Y. P. Shen, "Hydrology and water resources variation and its response to regional climate change in Xinjiang," *J. Geograph. Sci.*, vol. 20, no. 4, pp. 599–612, Aug. 2010.

[33] Y. Wang et al., "Methodology for mapping the ecological security pattern and ecological network in the arid region of Xinjiang, China," *Remote Sens.*, vol. 15, no. 11, May 2023, Art. no. 2836.

[34] C. Q. Han, J. H. Zheng, J. Y. Guan, D. L. Yu, and B. B. Lu, "Evaluating and simulating resource and environmental carrying capacity in arid and semiarid regions: A case study of Xinjiang, China," *J. Cleaner Prod.*, vol. 338, Mar. 2022, Art. no. 130646.

[35] Y. Q. Cheng et al., "Assessment and prediction of landscape ecological risk from land use change in Xinjiang, China," *Land*, vol. 12, no. 4, Apr. 2023, Art. no. 895.

[36] Z. P. Zhang, F. Q. Xia, D. G. Yang, J. W. Huo, G. L. Wang, and H. X. Chen, "Spatiotemporal characteristics in ecosystem service value and its interaction with human activities in Xinjiang, China," *Ecol. Indicators*, vol. 110, Mar. 2020, Art. no. 105826.

[37] C. Cao, Y. T. Luo, L. P. Xu, L. Y. Xi, and Y. M. Zhou, "Construction of ecological security pattern based on InVEST-Conefor-MCRM: A case study of Xinjiang, China," *Ecol. Indicators*, vol. 159, Feb. 2024, Art. no. 111647.

[38] T. Wang, Z. P. Yang, F. Han, J. B. Yu, X. K. Ma, and J. L. Han, "Assessment of tourism socio-ecological system resilience in arid areas: A case study of Xinjiang, China," *Ecol. Indicators*, vol. 159, Feb. 2024, Art. no. 111748.

[39] Z. Kulaixi, Y. N. Chen, C. Wang, and Q. Q. Xia, "Spatial differentiation of ecosystem service value in an arid region: A case study of the Tarim River Basin, Xinjiang," *Ecol. Indicators*, vol. 151, Jul. 2023, Art. no. 110249.

[40] Z. H. Xu et al., "Evaluation and simulation of the impact of land use change on ecosystem services based on a carbon flow model: A case study of the Manas River Basin of Xinjiang, China," *Sci. Total Environ.*, vol. 652, pp. 117–133, Feb. 2019.

[41] S. Li, J. Li, H. Wang, Z. Yang, X. Liu, and C. Lei, "Impact of transport superiority on ecosystem health in arid regions: A case study of southern Xinjiang, China," *Ecol. Indicators*, vol. 162, May 2024, Art. no. 112054.

[42] X. B. Dong, W. K. Yang, S. Ulgiati, M. C. Yan, and X. S. Zhang, "The impact of human activities on natural capital and ecosystem services of natural pastures in North Xinjiang, China," *Ecol. Model.*, vol. 225, pp. 28–39, Jan. 2012.

[43] Y. Liu, W. Hu, S. W. Wang, and L. Y. Sun, "Eco-environmental effects of urban expansion in Xinjiang and the corresponding mechanisms," *Eur. J. Remote Sens.*, vol. 54, pp. 132–144, Mar. 2021.

[44] R. R. Liu, X. B. Dong, X. C. Wang, P. Zhang, M. X. Liu, and Y. Zhang, "Relationship and driving factors between urbanization and natural ecosystem health in China," *Ecol. Indicators*, vol. 147, Mar. 2023, Art. no. 109972.

[45] J. H. Zhou et al., "Estimation of aboveground biomass of senescence grassland in China's arid region using multi-source data," *Sci. Total Environ.*, vol. 918, Mar. 2024, Art. no. 170602.

[46] G. Y. Wang, J. F. Mao, L. L. Fan, X. X. Ma, and Y. M. Li, "Effects of climate and grazing on the soil organic carbon dynamics of the grasslands in Northern Xinjiang during the past twenty years," *Glob. Ecol. Conservation*, vol. 34, Apr. 2022, Art. no. e02039.

[47] K. J. Cao and J. Gao, "Assessment of climatic conditions for tourism in Xinjiang, China," *Open Geosci.*, vol. 14, no. 1, pp. 382–392, Apr. 2022.

[48] X. L. Yuan, J. Bai, L. H. Li, A. Kurban, and P. De Maeyer, "The dominant role of climate change in determining changes in evapotranspiration in Xinjiang, China from 2001 to 2012," *PLoS One*, vol. 12, no. 8, Aug. 2017, Art. no. e0183071.

[49] B. D. Sun, J. C. Tang, D. H. Yu, Z. W. Song, and P. G. Wang, "Ecosystem health assessment: A PSR analysis combining AHP and FCE methods for Jiaozhou Bay, China," *Ocean Coastal Manage.*, vol. 168, pp. 41–50, Feb. 2019.

[50] M. Izadikhah, A. Saeidifar, and R. Roostaee, "Extending TOPSIS in fuzzy environment by using the nearest weighted interval approximation of fuzzy numbers," *J. Intell. Fuzzy Syst.*, vol. 27, no. 6, pp. 2725–2736, 2014.

[51] Y. A. Solangi, Q. M. Tan, N. H. Mirjat, and S. Ali, "Evaluating the strategies for sustainable energy planning in Pakistan: An integrated SWOT-AHP and fuzzy-TOPSIS approach," *J. Cleaner Prod.*, vol. 236, Nov. 2019, Art. no. 117655.

[52] Ö. Ekmekcioglu, K. Koc, and M. Özger, "Stakeholder perceptions in flood risk assessment: A hybrid fuzzy AHP-TOPSIS approach for Istanbul, Turkey," *Int. J. Disaster Risk Reduction*, vol. 60, Jun. 2021, Art. no. 102327.

[53] J. F. Wang, T. L. Zhang, and B. J. Fu, "A measure of spatial stratified heterogeneity," *Ecol. Indicators*, vol. 67, pp. 250–256, Aug. 2016.

[54] X. L. Wang, S. H. Shi, X. Zhao, Z. R. Hu, M. Hou, and L. Xu, "Detecting spatially non-stationary between vegetation and related factors in the Yellow River Basin from 1986 to 2021 using multiscale geographically weighted regression based on Landsat," *Remote Sens.*, vol. 14, no. 24, Dec. 2022, Art. no. 6276.

[55] C. L. Xue, X. H. Chen, L. R. Xue, H. Q. Zhang, J. P. Chen, and D. D. Li, "Modeling the spatially heterogeneous relationships between tradeoffs and synergies among ecosystem services and potential drivers considering geographic scale in Bairin Left Banner, China," *Sci. Total Environ.*, vol. 855, Jan. 2023, Art. no. 158834.

[56] S. Tong et al., "Spatiotemporal drought variability on the Mongolian Plateau from 1980-2014 based on the SPEI-PM, intensity analysis and Hurst exponent," *Sci. Total Environ.*, vol. 615, pp. 1557–1565, Feb. 2018.

[57] A. Yushanjiang, F. Zhang, and M. L. Tan, "Spatial-temporal characteristics of ecosystem health in Central Asia," *Int. J. Appl. Earth Observ. Geoinf.*, vol. 105, Dec. 2021, Art. no. 102635.

[58] J. Yao et al., "Hydro-climatic changes and their impacts on vegetation in Xinjiang, Central Asia," *Sci. Total Environ.*, vol. 660, pp. 724–732, Apr. 2019.

[59] X. L. Tang, X. Lv, and Y. He, "Features of climate change and their effects on glacier snow melting in Xinjiang, China," *Comptes Rendus Geosci.*, vol. 345, no. 2, pp. 93–100, Feb. 2013.

[60] C. Chen et al., "China and India lead in greening of the world through land-use management," *Nature Sustainability*, vol. 2, no. 2, pp. 122–129, Feb. 2019.

[61] C. Jiang, F. Wang, H. Y. Zhang, and X. L. Dong, "Quantifying changes in multiple ecosystem services during 2000-2012 on the Loess Plateau, China, as a result of climate variability and ecological restoration," *Ecol. Eng.*, vol. 97, pp. 258–271, Dec. 2016.

[62] H. Wei et al., "Linking ecosystem services supply, social demand and human well-being in a typical mountain-oasis-desert area, Xinjiang, China," *Ecosyst. Serv.*, vol. 31, pp. 44–57, Jun. 2018.

[63] R. R. Liu, X. B. Dong, P. Zhang, Y. Zhang, X. W. Wang, and Y. Gao, "Study on the sustainable development of an arid basin based on the coupling process of ecosystem health and human wellbeing under land use change—A case study in the Manas River Basin, Xinjiang, China," *Sustainability*, vol. 12, no. 3, Feb. 2020, Art. no. 1201.

[64] D. W. Dong, H. Tao, and Z. X. Zhang, "Projected population exposure to heatwaves in Xinjiang Uygur autonomous region, China," *Sci. Rep.*, vol. 14, no. 1, Feb. 2024, Art. no. 4570.

[65] J. Peng, Y. X. Liu, T. Y. Li, and J. S. Wu, "Regional ecosystem health response to rural land use change: A case study in Lijiang City, China," *Ecol. Indicators*, vol. 72, pp. 399–410, Jan. 2017.

Xiaming Yang is currently working toward the M.Sc. degree in ecology with Xinjiang University, Urumqi, China.

His research interests include ecosystem health and ecosystem services research.

Renping Zhang received the B.S. degree in grassland Science from Gansu Agricultural University, Lanzhou, China, in 2004, the M.S. degree in forest manager from Shihezi University, Shihezi, China, in 2007, and the Ph.D. degree in herbology from Lanzhou University, Lanzhou, in 2017.

He is currently a Faculty Member of the Department of Ecology, College of Ecology and Environment, Xinjiang University, Urumqi, China. He also serves as an expert in assessing the assessment of national greenhouse gas voluntary emission reduction transactions, an expert in assessing the registration of natural resources in Xinjiang, an expert in assessing the accounting of carbon sinks of the Department of Ecology and Environmental Protection, an expert in reviewing the grassland expropriation and occupation in Xinjiang Autonomous Region, an expert in assessing the investment projects of the government of Urumqi, and a general technical guide of the grassland fire census in the autonomous region. His main research interests include using remote sensing data to study grasslands, snow depth and their response to climate change in Xinjiang, as well as exploring ecosystem carbon sources and sinks and forest fires.

Jing Guo received the B.S. degree in grassland Science and M.S. degrees in forest manager in 2006 and 2009, respectively, from Xinjiang Agricultural University, Urumqi, China, where she is currently working toward the Ph.D. degree in resources and environment at Xinjiang University, Xinjiang, China.

Since 2011, she has been an Assistant Researcher with the Xinjiang Forestry Academy of Sciences, Urumqi, where her main research interests include remote sensing of forests and climate change in Xinjiang as well as the impacts of low-temperature freezes on the forest and fruit industries.

Liangliang Zhang is currently working toward the Resources and Environment Program degree in ecology with Xinjiang University, Urumqi, China.

His research interests include forest and grassland fire studies.

Xueping Gou is currently working toward the M.Sc. degree in ecology with Xinjiang University, Urumqi, China.

Her research interests include grassland vegetation cover studies.

Zhengjie Gao is currently working toward the Resources and Environment Program degree in ecology with Xinjiang University, Urumqi, China.

His research interests include the study of forest and forest carbon sinks.

Xuewei Liu is currently working toward the M.Sc. degree in ecology with Xinjiang University, Urumqi, China.

Her research interests include grassland carbon sink studies.